

Technical Evaluation of a Fiber-Optic Probe Dissolution System

Li Liu^{1,3}, Gifford Fitzgerald², Matthew Embry¹, Ricardo Cantu¹, and Brian Pack¹

e-mail: LIU_LI_X1@LILLY.COM

¹ Eli Lilly and Company, Indianapolis, IN 46285.

² University of Notre Dame, Chemistry Department, South Bend, IN 46556.

ABSTRACT

A systematic investigation was performed on the Delphian Rainbow Dissolution Monitor[®] to fully characterize the analytical performance of this instrument. The spectra of more than thirty commonly used pharmaceutical excipient samples were analyzed and grouped into three categories based on their UV absorbance or scattering properties. Scattering interference from the insoluble excipients is unique to the UV fiber-optic in situ analysis, since all components are present during the analysis; therefore, it was further evaluated for its impact on accuracy, linearity, and precision. The simple baseline-correction algorithm worked well to minimize spectral interference derived from excipient scattering because of the fact that scattering is mostly wavelength independent for the excipients studied in this work. The baseline-corrected spectra demonstrated that the presence of insoluble excipients did not have significant impact on linearity or accuracy. However, increased variability in the presence of insoluble excipients led to an increase in the minimum measurable absorbance from 0.03 to 0.05 absorbance units (AU), which ultimately limits low-level quantitative measurements. Assessment of four different path lengths showed consistent linearity in the operational range of 0.05–1.5 AU. The linear range was observed to decrease at shorter wavelengths (240-nm cutoff) due to the lack of full transmittance, which is consistent with the specification defined by the manufacturer. In addition, practical recommendations are provided to allow the user to get the most accurate data from the system.

INTRODUCTION

UV fiber-optic dissolution is gaining acceptance as a powerful technique in the pharmaceutical industry. Although still in the early stages of being accepted in a quality control environment, it is becoming a mainstay technique to support product development from candidate selection through acceptance of market formulation. The technique has received much attention since Josefson and others (1) applied it to tablet dissolution testing in the late 1980s. Other reports in the literature describe subsequent improvements in hardware and data treatment (2–4). Since commercial UV fiber-optic dissolution instruments became available in late 1990s, there have been many evaluations to investigate hydrodynamic effects (5–7), linear range (5, 6), precision (6), excipient impact (5, 8, 9), air bubble impact (5, 10), and scattering correction methods (8, 10).

Among its many inherent advantages, in situ spectrophotometric measurement eliminates the need for manual sampling and the subsequent off-line analysis typically conducted by conventional chromatography or UV–VIS solution analysis. Most importantly, real-time and rapid data collection provides a wealth of information depicting detailed and complete drug release profiles during the course of a dissolution experiment. This attribute can offer significant insight into the release profile of a drug product when compared with the

conventional off-line analysis where relatively few data points can be generated.

Some unique characteristics are associated with the hardware of the fiber-optic dissolution system. Unlike conventional off-line analysis when discreet samples are placed, or elute, in the light path between the lamp and the detector, the fiber-optic system relies on the optical fibers to transfer the light from the source to the probes and carry the non-absorbed light back to the detector. The lack of full transmittance may occur in a certain wavelength range; this reduces the amount of available light and therefore may reduce the detector linear range and increase the limit of quantitation (6, 11). In addition, the path length can be altered on each probe by simply utilizing a different probe tip. Probes have mirrors that reflect the light back to the detector through the fiber-optic cables and have the potential to introduce stray light and reduce the method linear range (6). Since the amount of stray light can vary with different path lengths, the linear range could be impacted differently for different path length probes.

The largest obstacle for UV fiber-optic dissolution is the presence of insoluble excipients that flow around and through the flow cell and may cause scattering and the blockage of light. It is known that the scattering generated by insoluble excipients can contribute significant interference. There are two type of scattering interference (5, 8). The first type is wavelength-independent; this is observed more frequently and manifests itself by a baseline offset over the entire UV range. The second type

³Corresponding author.

of scattering event is wavelength-dependent and produces a sloped baseline with increased offset towards the lower wavelength region. This type of scattering is known as Tyndall scattering and is observed in colloidal suspensions (extremely small particle size). The first type of scattering can be corrected by simple baseline correction algorithms (e.g., subtracting the absorbance at a selected reference wavelength). The second type of scattering correction requires more complicated mathematical approaches such as a second-derivative algorithm.

In the literature, the assessments of the fiber-optic dissolution systems were performed primarily by evaluating linear ranges at a specified path length and precision at selected concentrations or by using real time dissolution data. The assessments for excipients were typically conducted by comparing the UV fiber-optic on-line results with those obtained from the conventional off-line UV analysis for real time dissolution of selected pharmaceutical drug products.

The main objective of this work was to evaluate commonly used pharmaceutical excipients systematically to understand their impact on accuracy, linear range, and limit of quantitation. Thirty-five excipient samples were selected for this evaluation. In addition, five drug product placebos that closely resembled the active pharmaceutical products were assessed. A Delphian Rainbow Dissolution® system was used for the studies. The evaluation was performed using excipients and standards alone (i.e., no release profiles were generated) to understand the fundamental figures of merit, such as consistency between six probes and four path lengths, and the minimum required absorbance that corresponds to limit of quantitation (LOQ).

Hydralazine hydrochloride was selected as a model compound because of its desirable UV spectrum as shown in Figure 1. The spectrum of the compound provides

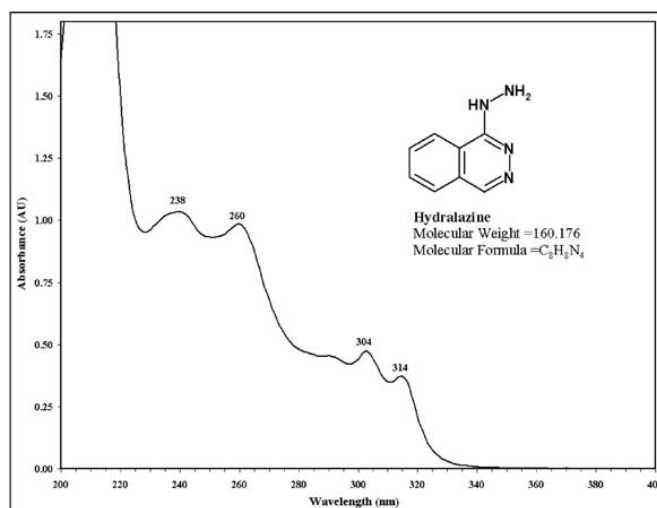


Figure 1. UV absorbance spectrum of hydralazine HCl (0.02 mg/mL in 0.001 N HCl).

relatively consistent absorbance from 238 to 260 nm and from 270 to 314 nm. In addition, it has four local UV maxima at 238, 260, 304, and 314 nm. Such a UV profile allows a compound-independent assessment of the impact of wavelength on instrument performance or data analysis. Therefore, additional molecule-specific variables were not introduced into the evaluation. To focus on instrument capabilities, the model compound served as a surrogate, and the quantitative results were expressed as UV absorbance rather than compound-specific concentrations. Hydralazine is very soluble in aqueous media and is stable in the sample solvent or dissolution medium selected in this work.

EXPERIMENTAL

Instrumentation

A Rainbow Dynamic Dissolution Monitor® system from Delphian Technology Inc. (Woburn, MA, USA) was utilized with a dissolution system (VK 7025) from Varian. An 8453 UV-visible spectrometer from Agilent Technologies (Palo Alto, CA, USA) was utilized for the offline UV determinations.

Chemicals and Materials

Hydralazine hydrochloride and 0.1 N hydrochloric acid were obtained from Sigma-Aldrich Co. (St. Louis, MO, USA). Deionized water was obtained from an in-house supply. The excipient information is summarized in Table 1. The ingredients for the placebos are summarized in Table 2. The placebos were manufactured by a wet-granulation process.

Evaluation of System Linearity

Standard solutions of hydralazine hydrochloride were prepared in 0.001 N HCl at concentrations encompassing the expected linear absorbance range. Therefore, the ranges are deliberately specific to each of the four available probe tip path lengths assessed. Sixteen standards were prepared from 3 to 170 µg/mL for the 2-mm path length. Eleven standards were prepared from 2.4 to 112 µg/mL for the 5-mm path length. Twenty standards were prepared from 0.6 to 40 µg/mL for the 10-mm path length. Fifteen standards were prepared from 0.2 to 20 µg/mL for the 20-mm path length. All standards were prepared by serial dilution. The standards prepared for 10-mm path length were also measured in the Agilent UV-visible spectrometer using a 10-mm path length.

The linear range was also assessed as a function of wavelength utilizing the 20-mm path length. Additional standard solutions were prepared (i.e., 8–40 µg/mL) to accommodate different extinction coefficients of hydralazine across the wavelength range so that the assessment could be performed across the entire linear absorbance range. The absorbances of the standard solutions were measured in 20-mL scintillation vials from six probes, and a single scan was collected for each concentration.

Table 1. Excipient Information.^a

Excipient	Manufacturer	Category ^b
Lactose	Foremost Farms, Rothschild, WI (Supplier CHR Hansen Inc. Milwaukee, WI)	1
Lactose spray-dried special	Foremost Farms, Rothschild, WI (Supplier CHR Hansen Inc. Milwaukee, WI)	
Mannitol Parenteral	Roquette Freres Lestem, France	
Mannitol USP Pearlitol SD-200	Roquette Freres Lestem, France	
Mannitol Pearlitol SD-100	Roquette Freres Lestem, France	
PEG 3350	Dow Chemical Company Hahnville, LA 70057	
Hydroxyl propyl cellulose EF	Hercules Inc., Aqualon Div. Hopewell, VA	
Hydroxyl propyl methyl cellulose 5	Dow Chemical Co. Midland, MI (Supplier Univar USA Inc. Indianapolis, IN)	
Maltodextrin Lycatab DSH	Roquette Freres Lestem, France	
Sodium lauryl sulfate	Stepan Chemical Co. Northfield, IL	
Poloxamer-188	BASF Corporation Florham Park, NJ 07932	
Microcrystalline cellulose (MCC)	Penwest Pharmaceuticals Cedar Rapids, IA	2
MCC granular-102	FMC Corp. Newark, DE	
MCC granular-302	FMC International Wallingstown Cork Ireland	
Starch flowable powder	Colorcon West Point, PA	
Starch flowable with 5% silicone	Eli Lilly & Co.	
Partially pregelatinized starch	Roquette Freres Lestem, France	
Dibasic calcium phosphate dihydrate	Sigma Chemical Corp. St. Louis, MO	
Dibasic calcium phosphate anhydrous	Sigma Chemical Corp. St. Louis, MO	
Crospovidone XL	International Specialty Products, Calvert City, KY	
Crospovidone XL-10	International Specialty Products, Calvert City, KY	
Sodium croscarmellose	FMC Biopolymer Div. Newark, NJ	
Sodium starch glycolate	Roquette Freres Lestem, France	
Magnesium stearate vegetable	Mallinckrodt Inc. St. Louis, MO	
Stearic acid powder	Witco Corp., Humko Div. Memphis, TN	
Colloidal silicon dioxide	Cabot Corp. Tuscola, IL (Supplier Mays Chemical Co. Inc., Indianapolis, IN)	
Talc extra fine	IMI FABI LLC Benwood, WV (Supplier WLS Enterprises Inc., Indianapolis, IN)	
Opadry [®] II PVA based	Colorcon West Point, PA	
HPMC capsule shells	Shionogi	
Povidone	International Specialty Products, Texas City, TX	
Polysorbate 80 vegetable	Croda Inc. Mill Hall, PA	
Vitamin E-TPGS	Eastman Chemical Company USA, Kingsport, TN 37662	
Swedish orange gelatin capsule shells (lot C40307)	Capsugel Greenwood, SC	
Shionogi opaque white gelatin capsule shells (lot N0502891)	Shionogi Qualicaps, Inc. Whitsett, NC	
Blue opaque gelatin capsule shells (Lot 640739)	Capsugel Greenwood, SC	

^a The solubility assessment was based on visual observation.

^b Category Descriptions:

1 Soluble excipients with UV cutoff < 240 nm

2 Insoluble excipients

3 Soluble or partially soluble excipients with UV cutoff ≥ 240 nm

Table 2. Composition of Placebos.

	Tablet Lot				Granulation Lot
	A	B	C	D	E
Intra-Granular Ingredients (mg/unit formula)					
Lactose spray-dried special	413.6				
Microcrystalline cellulose granular-102	41.4	41.1	70.9	70.9	111.0
Pearlitol 100 SD		411.4			
Mannitol			212.6	212.6	333.0
Hydroxy propyl cellulose EF Extra Fine	15.0				
Hydroxy propyl methyl cellulose 5		15.0			
Povidone			14.0	14.0	19.2
Sodium croscarmellose	15.0	15.0	7.0		
Crospovidone XL				7.0	14.4
Extra-granular Ingredients (mg/unit formula)					
Magnesium stearate vegetable	5.0	2.5	3.5	3.5	2.4
Hydroxy propyl cellulose EF					
Sodium croscarmellose	10.0	10.0	7.0		
Microcrystalline cellulose granular-102			35.0	35.0	
Crospovidone XL				7.0	
Total (mg)	500	500	350	350	480

Evaluation of System Limit of Quantitation

Standard solutions of hydralazine hydrochloride were prepared in 0.001 N HCl at concentrations of 0.2, 0.3, 0.6, and 0.75 µg/mL and transferred to 20-mL scintillation vials for measurement using a 20-mm path length. For each concentration, 13 scans were collected on all six probes at five-minute intervals over the course of an hour. The relative standard deviation (RSD) was calculated for the 13 measurements for each individual probe. The RSD was also calculated across the six probes to determine the inter-probe variability.

Evaluation of Interferences Caused by Common Excipients

For each experimental run, six excipients were weighed and transferred into six dissolution vessels. One liter of pre-heated 0.001 N HCl was then transferred into each vessel. Testing was performed using USP Apparatus II (paddles) at 50 rpm. Approximately 15–20 scans were collected at a frequency of one scan per minute using a 20-mm path length.

The weight of each targeted excipient was established based upon excipient functionality in a typical formulation. For example, in a 500-mg unit formula, the excipient used as the filler would likely be present at the highest level. Therefore, 500 mg of the excipients

commonly used as fillers was tested. This amount is equivalent to 100% of the assumed unit formula. Disintegration agents, binders, and film coatings were all tested at 30 mg, which represents approximately 6% of the assumed unit formula. Likewise, 20 mg of lubricants was tested to represent the equivalent of 4% of the assumed unit formula.

Evaluation of the Presence of Excipients on Linearity and Limit of Quantitation

The design of this experiment involved a side-by-side comparison of hydralazine standards with the excipient-spiked standards, both prepared in triplicate. The three excipients selected for this experiment were starch, microcrystalline cellulose, and placebo lot B. The samples were prepared by transferring 1000 mL of pre-heated 0.001 N HCl into six dissolution vessels, three of which contained 500 mg of the selected excipient samples. The placebo tablets were dropped into the medium at the beginning of the run. Stock hydralazine standards were prepared at concentrations of approximately 1.0 and 0.1 mg/mL to produce appropriate hydralazine concentrations in situ. For each standard concentration, one of the stock hydralazine standards was added to each of the six vessels at the predetermined volume. Fourteen standard concentrations were prepared over the range of

0.15–15 µg/mL. Testing was conducted using USP Apparatus II (paddles) at 50 rpm. The 0.001 N HCl dissolution medium was helium sparged prior to use. Approximately 6–10 scans were collected at a frequency of one scan per minute using the 20-mm path length.

RESULTS AND DISCUSSION

Evaluation of System Linearity

Figure 2a displays hydralazine absorbance versus concentration for the path lengths of 2 mm, 5 mm, 10 mm, and 20 mm. Each data point represents the average absorbance of six probes. The error bars show the variability of the response across the six probes. The response curve for each of the four path lengths was found to be linear below 1.5 absorbance units (AU). Therefore, the linear equations in the figure were derived only for data points below 1.5 AU. When the absorbance

exceeded 1.5 AU, response deviated from linearity significantly, and the precision decreased as indicated by an increase in the size of the error bars. To estimate the percent deviation from linearity, a calculation was performed for the 20-mm path length using the ratio between the residual and the nominal absorbance obtained from the fitted linear curve. The deviation was found to be approximately 11% when the response reached approximately 2.0 AU.

For the purpose of performing a path-length comparison, the slopes of the 10-mm, 5-mm, and 2-mm path lengths were normalized to the slope of 20-mm path length, by applying factors of 2, 4, and 10, respectively. The normalized slopes were found to be 105.1 for the 20-mm path length, 107.1 for the 10-mm path length, 107.1 for the 5-mm path length, and 118.2 for the 2-mm path length. Although there was about 10% deviation between the slope of the 2-mm path length and those of the other path lengths, this discrepancy was found to have no impact on the data analysis where the ratio of sample absorbance and standard absorbance is used for the percent released calculation in a typical dissolution experiment. To illustrate this point, Figure 2a was rearranged into Figure 2b. Figure 2b displays the linear plot of each path length using the absorbance ratio of an absorbance versus the absorbance at a selected concentration. To compare the data on the same scale for different path lengths, the concentrations were normalized to 20-mm path length using the equation $C_2 = C_1/(b_2/b_1)$, where C_1 and C_2 represent concentrations before and after normalization, and b_2 and b_1 represent 20 mm and the path length to be normalized, respectively. The normalization factor b_2/b_1 was determined to be 2, 4, and 10 for the path lengths of 10 mm, 5 mm, and 2 mm, respectively. Figure 2b demonstrates that consistent linearity is achieved among all four path lengths. Therefore, the data suggest that there is no significant difference in the impact of stray light for the different path lengths. Based upon this result, the linearity established for one path length can be applied to probes with different path lengths. Therefore, when more than one path length is required to encompass a range of dose strengths, the evaluation of linearity for one path length may be sufficient provided that the same absorbance range is achieved.

The Delphian fiber-optic dissolution system is reported to have a UV cutoff at approximately 240 nm due to the lack of full transmittance below this wavelength. The impact of wavelength on accuracy and precision was evaluated for multiple wavelengths including 238, 250, 260, 280, 304, and 314 nm. The linear plots from those wavelengths are illustrated in Figure 3. Each data point was taken from the average absorbance of six probes. The error bars illustrate the variability that was observed between the probes. To compare the data on the same

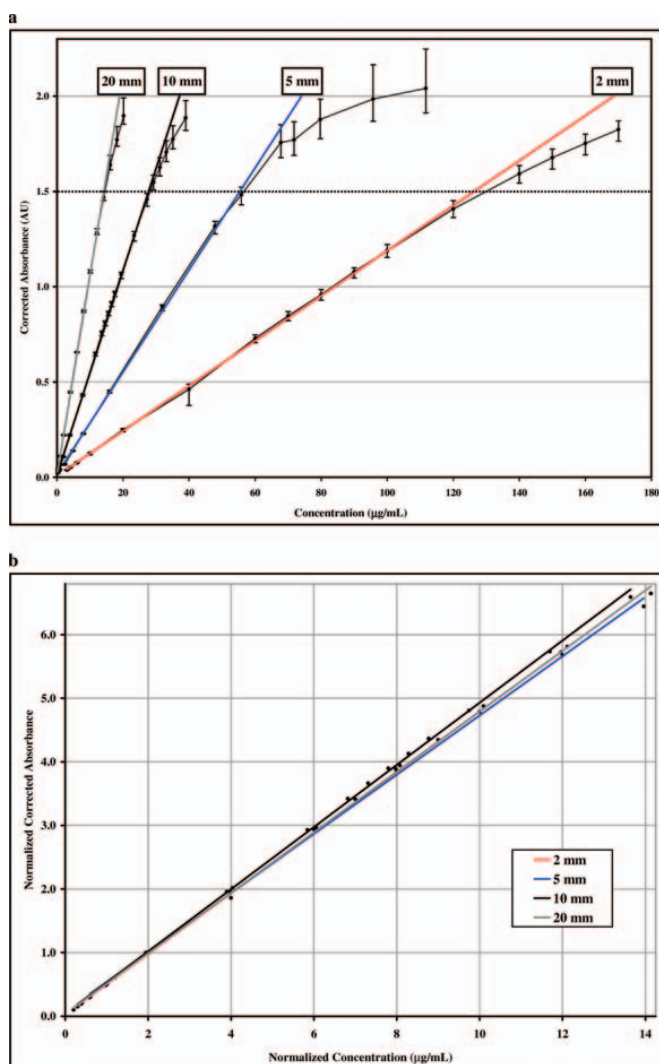


Figure 2. Comparison of linearity for path lengths of 2, 5, 10, and 20 mm at 260 nm using hydralazine HCl. (a) Absorbance and concentration not normalized. (b) Absorbance normalized to a selected absorbance; concentration normalized to 20-mm path length.

scale for different wavelengths, the concentrations were normalized to 260 nm using the equation $C_2 = C_1 / (\epsilon_2/\epsilon_1)$ where C_1 and C_2 represent concentrations before and after normalization, and ϵ_2/ϵ_1 represent the ratio of the extinction coefficient between 260 nm and the wavelength to be normalized. The average normalization factor ϵ_2/ϵ_1 was determined to be 0.95, 1.06, 2.04, 2.12, and 2.64 for 238, 250, 280, 304, and 314 nm, respectively. The results in Figure 3 show consistent performance between 250 and 314 nm. At 238 nm, however, the response deviated from linearity when the absorbance exceeded 1.0 AU. The error bars also started to increase in magnitude around 1.0 AU and the magnitude of the increase was proportional to the absorbance. The above data confirm that transmission losses at low wavelengths result in a decreased linearity range and an increase in variability.

The linearity data obtained from 10-mm fiber-optic probes were also compared with the results measured by a conventional UV spectrometer. The two linear curves were superimposable, indicating consistent measurements between the fiber-optic UV and the conventional UV.

Evaluation of System Limit of Quantitation

The system precision is known to be affected by the system noise level, which determines the minimum signal required for quantitative measurements. The concentration of a compound that corresponds to this minimum signal is the limit of quantitation (LOQ) for that compound. To make this a system evaluation as opposed to a compound-specific evaluation, an absorbance LOQ was established rather than a compound-specific LOQ. Thus, the LOQ reported here will apply to all compounds

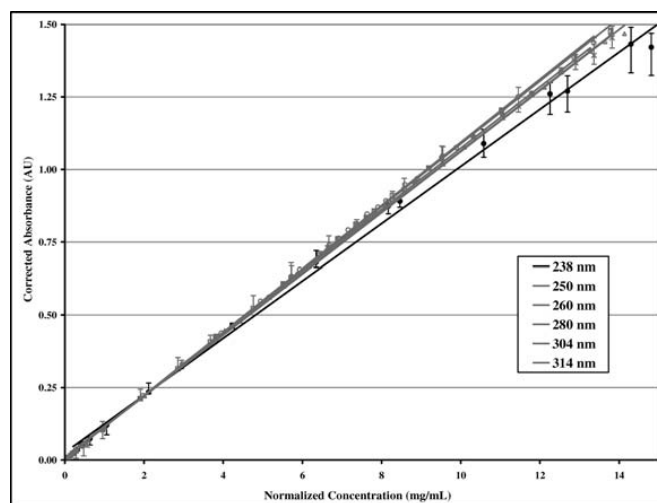


Figure 3. Comparison of linearity at multiple wavelengths using hydralazine HCl (concentration normalized using the ratio of extinction coefficients at the selected wavelength vs. 260 nm).

Table 3. Percent RSD at Low Absorption Levels that Represents the Absorbance LOQ of the System.

	Probe #	0.02 AU	0.03 AU
%RSD (n=13) Measurements for each probe	1	6.79%	1.19%
	2	4.36%	1.55%
	3	3.33%	1.08%
	4	2.10%	1.39%
	5	1.57%	1.09%
	6	4.90%	0.73%
%RSD for probes 1-6		12.57%	3.37%

that generate the reported absorbance values. The absorbance LOQ was assessed by finding the absorbance that corresponds to approximately 10% RSD. The RSD was calculated for 13 measurements from each individual probe. The RSD was also calculated across six probes to determine the inter-probe variability. The absorbance LOQ was determined to be 0.03 AU based on the data summarized in Table 3. Depending upon the molar absorptivity of the compound in question, this absorbance may correspond to drastically different concentrations in solution.

Evaluation of Interferences Caused by Common Excipients

Thirty-five excipient samples were analyzed including thirty single excipients, one excipient-mixture, and four capsule shells. In addition, one placebo granulation and four placebo tablets were studied. To represent the worst-case scenario in a typical dissolution experiment, the largest likely quantity of the excipient, based on a 500-mg fill weight and commonly used ranges of that excipient in a unit formula, was utilized. Each of the excipient samples was measured with the UV fiber-optic dissolution system, and the spectrum was evaluated. Three categories of excipients were defined based upon the nature of the interference caused by each excipient and are summarized in Table 1.

The first category is composed of soluble excipients that do not have a UV absorbance above 240 nm. These excipients will not cause interference, since the system has a UV cutoff at 240 nm and, therefore, will only be operated above 240 nm. However, these excipients may pose interferences if a different brand or model of instrument is used with a UV cutoff below 240 nm.

The second category contains insoluble excipients. These excipients cause scattering events that diminish the amount of light that reaches the detector. Figure 4 illustrates four representative samples including single

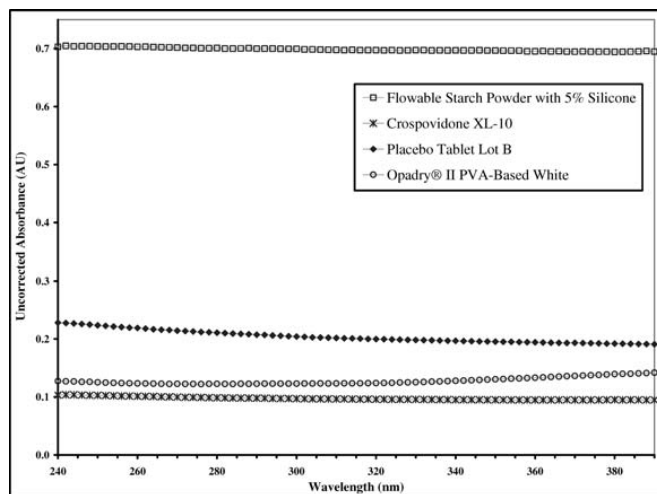


Figure 4. Insoluble excipient interference.

component excipients (i.e., starch and crospovidone), a placebo tablet (see Table 2 for composition), and a mixture (Opadry®II). The first three scattering spectra are characterized by a flat baseline offset across the entire wavelength range, with a minimal increase at shorter wavelengths. These characteristics were found in common

for all the excipients in this category except for Opadry®II. Two types of scattering interference that can impact a UV fiber-optic analysis have been described in the literature (5, 8). The first type is wavelength-independent and is characterized by a consistent baseline offset across the entire wavelength range. The second type of scattering interference, referred to as Tyndall scattering, is wavelength-dependent and is characterized by a sloped baseline with increased intensity towards the shorter wavelengths. The scattering observed for Opadry®II is wavelength-dependent, but in contrast to the Tyndall scattering pattern, Opadry®II showed a slight increase in scattering at longer wavelengths. The characteristics of the scattering profiles are summarized in Table 4. The data in the table show that the baseline offsets among the studied excipients range from <0.05 to 0.7 AU, reflecting low to high scattering levels. The data also show that the baseline offset caused by scattering is mostly wavelength-independent, as indicated by relatively small difference (referred as Δ in the table) in absorbance between 240 nm and 400 nm (i.e., $\Delta \leq 0.02$ AU). The small deltas for the most common insoluble excipients make it possible to effectively minimize the impact of scattering on accuracy by using a simple baseline-correction algorithm.

Table 4. Scattering Characteristics of Insoluble Excipients.

Baseline Offset (AUS)	Δ Absorbance (240–400 nm) AUS	Excipient	Concentration (mg/mL)
0–0.05	0–0.015	Colloidal silicon dioxide	0.018
		Dicalcium phosphate (anhydrous)	0.51
		Sodium starch glycolate	0.036
		Stearic acid powder	0.019
		Talc	0.019
0.05–0.1	0.005–0.01	Crospovidone XL	0.033
		Crospovidone XL-10	0.031
		Sodium Croscarmellose	0.034
0.1–0.2	0–0.015	MCC Granular – 102	0.51
		MCC Granular – 302	0.50
		Dicalcium phosphate (dihydrate)	0.51
		Magnesium stearate (vegetable)	0.019
		Shionogi HPMC	N/A – 1 capsule
0.1–0.2	–0.015	Opadry®II PVA-based white	0.035
0.2–0.3	0.008	MCC	0.51
0.3–0.4	0.015–0.02	Partially pregelatinized starch	0.51
0.5–0.7	0–0.015	Starch flowable powder w/5% silicone	0.51
		Starch flowable powder	0.51

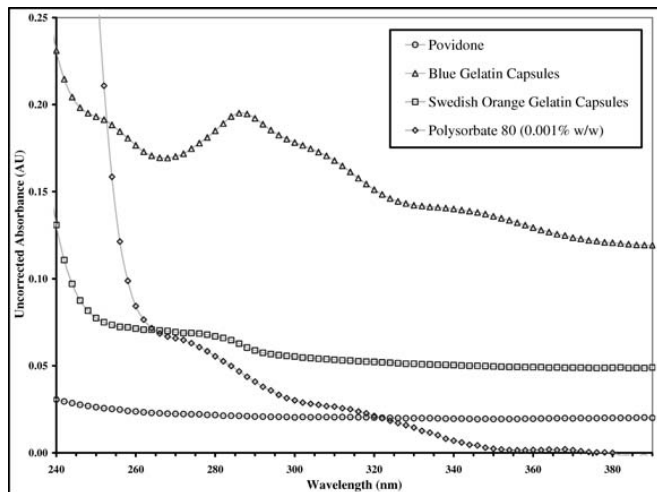


Figure 5. Excipients with UV interference.

The third category of excipients is composed of soluble or partially soluble excipients that absorb light at or above 240 nm. Figure 5 displays spectra for these excipients. Povidone has a UV cutoff near 240 nm and therefore did not present much interference from 240 to 400 nm. On the other hand, 0.001% Polysorbate 80 exhibited interference up to 350 nm. Gelatin capsule shells are partially insoluble and therefore showed baseline offset due to scattering and UV absorption. As expected, the resulting spectral interference was found to be additive (i.e., UV absorption plus scattering). The UV cutoff was around 290 nm for Swedish orange and opaque white gelatin capsule shells. The UV cutoff for blue gelatin capsule shells was 370 nm.

In summary, for most excipients, there are two main types of interferences that may result either from scattering or from UV absorption. The UV interference should be managed in the same manner as for any UV spectrometer. For example, fiber-optic dissolution may not be the best selection for a molecule that has an absorbance maximum at 290 nm and is present at a low level in a Swedish Orange capsule. The interference from insoluble excipients is unique and requires further investigation to understand whether the interference can be adequately corrected and the impact on the data analysis. The latter interference can ultimately impact the decision on the appropriateness of utilizing fiber-optic dissolution as opposed to filtered sampling.

Evaluation of the Presence of Excipients on Linearity and Limit of Quantitation

The previous data suggest that the scattering from insoluble excipients was mostly wavelength-independent. As a result, a simple baseline-correction algorithm is effective to remove the scattering interference. The baseline correction was conducted by subtracting the absorbance at a reference wavelength, which was 380 nm

in this work. To evaluate the impact of an excipient interference on linearity, accuracy, and precision, the design of the experiment involved side-by-side comparisons of standards with excipient-spiked standards in the linear range of 0.03–1.5 AU. Microcrystalline cellulose, starch, and a placebo tablet were evaluated. Microcrystalline cellulose and starch represent moderate- to high-scattering excipients. The placebo tablet, on the other hand, represents a wet-granulation processed tablet. The results from the three excipient samples show the same trend. Starch appears to represent the worst-case scenario and was therefore chosen as a representative example for the illustrations in Figures 6 and 7.

Figure 6 is an overlay of the baseline-corrected spectra of non-spiked and spiked standards from 1.5 to 14 $\mu\text{g/mL}$;

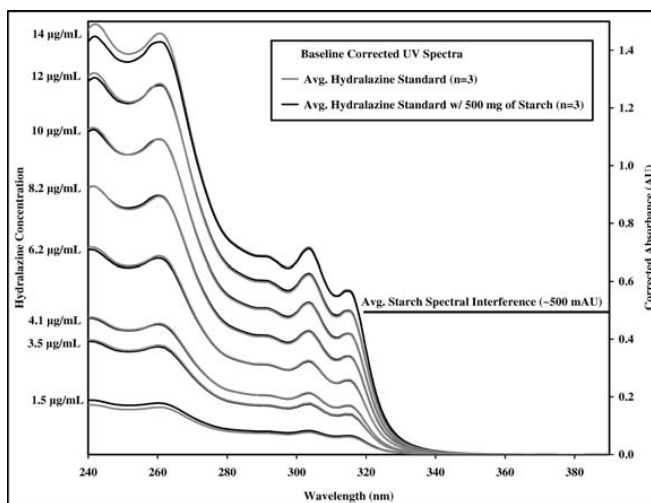


Figure 6. Comparison of baseline-corrected spectra of hydralazine standards and starch-spiked hydralazine standards.

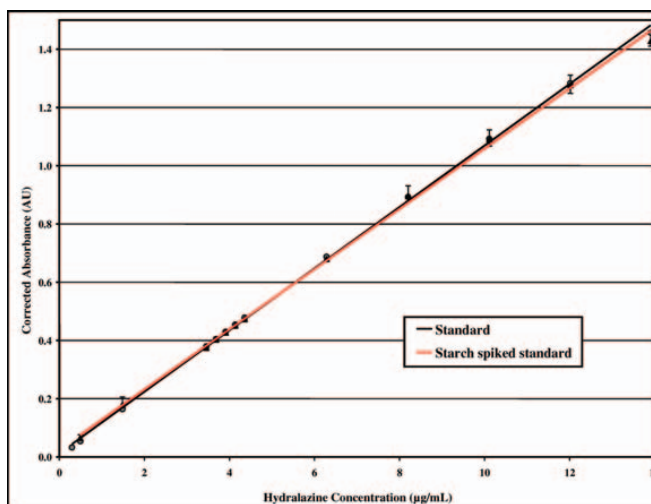


Figure 7. Impact of starch excipient on linearity and precision (using data at 260 nm).

this range corresponds to a UV absorbance of 0.2–1.5 AU. Data in Figure 6 show that the simple baseline-correction algorithm works well since the excipient-spiked spectra were comparable to the standard spectra, particularly when the absorbance was below 1.0 AU. At higher absorbances, the excipient-spiked standards show a decreased response. Such deviation from the standard was slightly larger as the absorbance increased. The percent deviation was calculated using the ratio between the excipient-spiked standard and the standard absorbance at which the deviation was observed. The largest percent deviation was 3% for starch and 2% for both the placebo tablet and microcrystalline cellulose. Errors around 2% are considered to be within the assay variability of a typical UV fiber-optic dissolution system. But it is important to understand all sources of error when analyzing dissolution profiles for multiple drug products. The slightly higher deviation from starch is thought to be correlated with its high scattering nature, which causes a baseline offset of 0.5 AU or higher. As a result, the total absorbance reached approximately 2.0 AU prior to the baseline correction. Figure 2a shows approximately 11% deviation (from the predicted line) for the 20-mm path length linearity curve at about 2.0 AU. When hydralazine produced a similar absorbance that accounted for approximately 1.5 AU and excipient scattering accounted for the remaining 0.5 AU, only 3% deviation was observed. The significantly lower level of error is unexpected and not yet understood. However, the results seem to suggest that the apparent absorbance caused by light scattering can be corrected adequately and, therefore, has a minimum impact on the linear range and accuracy.

Figure 7 is an overlay of the linearity curves of the starch-spiked and the non-spiked standards at 260 nm. Each data point represents the average absorbance of three fiber-optic probes. The error bars are displayed to estimate the variability from each probe (or vessel-to-vessel variability in real practice). For standard solutions, the error bars were found to be at least ten times smaller when compared with the spiked standards and were therefore considered negligible. Thus, only the error bars for spiked standards are shown in the graph so as not to complicate the figure. The results in Figure 7 demonstrate the consistent linearity between the spiked and the non-spiked standards. The error bars, on the other hand, exhibit increased noise in the presence of starch. To evaluate the absorbance LOQ in the presence of excipients, the RSD was summarized in Table 5 at low concentrations for the non-spiked and the starch-spiked standards. The results verify that the absorbance LOQ is 0.03 AU for the system and increases to 0.05 AU in the presence of starch. The absorbance LOQ of 0.05 AU should be acceptable for most commonly used excipients assuming starch represents the worst-case scenario due to its high scattering characteristics.

Table 5. Comparison of Percent RSD at Low Absorption Levels between Standard and Starch-Spiked Standard Illustrating Potential Negative Impact of Excipients on Low-Level Measurements.

	Probe	Standard		Starch + Standard	
		0.03 AU	0.05 AU	0.03 AU	0.05 AU
%RSD (n=13) measurements for each probe	1	0.13%	0.05%	2.14%	0.93
	2	0.18%	0.20%	14.00%	4.41
	3	0.26%	0.15%	8.91%	5.33
%RSD for probes 1–3		2.95%	1.79%	2.59%	2.44%

PRACTICAL CONSIDERATIONS: STANDARDIZATION, PROBE ORIENTATION, MEDIA DEGASSING

Standardization Recommendation

It is recommended to test the standard in a flask, beaker, or tube that has a minimum internal diameter of 25 mm. The probe dimensions will permit the use of narrow containers for measurement of standard solutions (e.g., 7-mL vials), which minimizes the required standard volume. However, accuracy is significantly sacrificed by such a practice. The ideal container should closely resemble the actual dissolution vessel. In practice, 20-mL scintillation vials (≈25 mm i.d.) gave acceptable results.

Probe Orientation Recommendation

Although not stated by the vendor, there is a preferred orientation of the fiber-optic probe in each vessel. Probe orientation has been previously investigated (12). A comparison of the optimized and non-optimized orientations was made for the percent release of 5-mg prednisolone tablets at 15, 30, 45, and 60 minutes. The results from this study were at 80% release or higher; the noise associated with the non-optimized orientation was a small fraction of the total absorbance, which shows that probe orientation has little effect.

However, Figure 8 demonstrates the impact of a common pharmaceutical excipient (i.e., starch) on the baseline-corrected background noise level for probes in two orthogonal orientations. Figure 8b illustrates the two probe orientations. In Figure 8a, the level of noise (peak-to-peak) is shown to be 2–3 times greater for the “non-optimized” orientation. Noise is approximated to be 7 mAU for the trace labeled “non-optimized” and 3 mAU for the trace labeled “optimized.” Additionally, the non-optimized trace shows spikes that are greater than 10 mAU in intensity. The level of noise is relevant to the absorbance LOQ that was cited earlier. Therefore, placement of the probes in the non-optimized orientation will increase the minimum quantifiable level by 7–10 mAU. These results were found to be very reproducible and were observed for all probes.

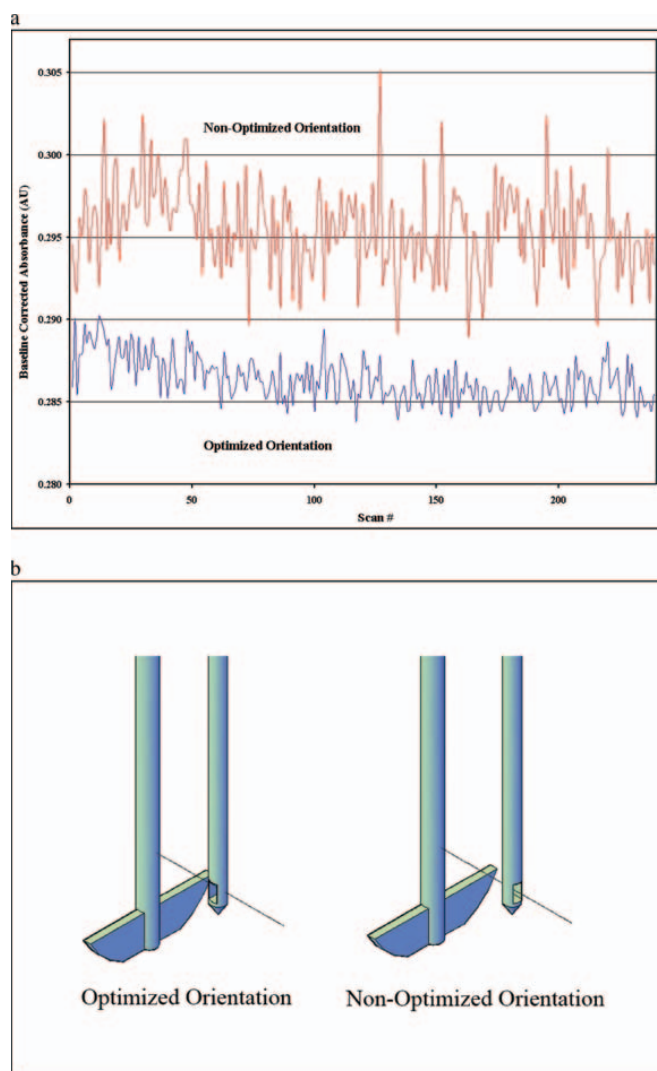


Figure 8. (a) Observed noise related to probe orientation in the presence of starch (500 mg in 1000 mL dissolution medium). (b) Probe orientation: optimized versus non-optimized.

The suspected cause of probe-orientation bias is the accumulation of light-scattering particulates in the optical path. In the optimized probe orientation, hydrodynamic flow continually moves particulates through the optical path so that the accumulation of flowing particulates is minimized. The results presented are specific to the fiber-optic probe design illustrated in Figure 8b and may not be applicable to other Delphian compatible probe designs.

Deaeration Recommendation

Thorough deaeration of the dissolution medium is strongly recommended even if the drug product is not sensitive to residual gas in the medium. A small bubble has the potential to produce a significant impact on UV light transmission if it finds its way into the optical path. As the medium is heated, small bubbles are commonly

observed to form on the apparatus shaft and probe surfaces even after moderate helium sparging. To avoid the formation of air bubbles, an appropriate deaeration technique should be performed with the medium at or above the temperature at which testing will be performed. If this is not possible because of the laboratory setup, careful monitoring for bubble formation should be made after the medium has reached temperature and prior to the start of a run.

CONCLUSION

This work evaluated 35 excipient samples and five placebos in the wavelength range of 240–400 nm using the Delphian fiber-optic dissolution system. The excipient profiles were grouped into three categories based on UV or scattering interferences. Soluble UV-active components, including Tween 80 and gelatin capsule shells, produced UV interference. Insoluble excipients created scattering interference, which is a unique problem associated with UV fiber-optic dissolution analysis since all components are present during the analysis. The resulting scattering spectra were characterized by baseline offsets across the entire UV range. The presence of insoluble particles and UV active components produced an additive spectrum.

The magnitude of the baseline offset varied with the type of excipient, but in general ranged from less than 0.05 to 0.7 AUFS. Those scattering spectra were relatively flat without significant slope offset from Tyndall scattering and, therefore, can be corrected with a simple baseline-correction algorithm. After the baseline correction, the standards spiked with excipients demonstrated comparable linear range when compared with the non-spiked standards.

Although insoluble excipients did not cause reduction for the upper linearity limit, their presence did increase the variability in the measurement at lower absorbance levels. Thus, the minimum absorbance required for the adequate quantitation was increased from 0.03 to 0.05 AUFS.

The fundamental evaluation of the fiber-optic system demonstrated consistent linearity across four path lengths and between the fiber-optic UV and a conventional off-line UV measurement in the range of 0.05–1.5 AUFS. However, the linear range was decreased, and variability was increased near 240 nm due to the loss of transmittance. In addition to the evaluation of the compound-independent figures of merit for this fiber-optic dissolution system, practical recommendations regarding standardization, probe alignment, and media degassing were made.

ACKNOWLEDGMENTS

The authors would like to acknowledge Jamie Veltri, Analytical Product Research and Development, and Melissa Keeney, Pharmaceutical Sciences Research and Development, for their insightful comments and contributions to this work.

References

1. Josefson, M.; Johansson, E.; Torstensson, A. Optical fiber spectrometry in turbid solutions by multivariate calibration applied to tablet dissolution testing. *Anal. Chem.* **1988**, *60*, 2666–2671.
2. Brown, C. W.; Lin, J. Interfacing a fiber optic probe to a diode array UV-visible spectrophotometer for drug dissolution tests. *Appl. Spectrosc.* **1993**, *47*, 615–618.
3. Chen, C-S.; Brown, C. W. A drug dissolution monitor employing multiple fiber optic probes and a UV/Visible diode array spectrophotometer. *Pharm. Res.* **1994**, *11* (7), 979–983.
4. Cho, J. H.; Gemperline, P. J.; Salt, A.; Walker, D. S. UV/Visible spectral dissolution monitoring by in situ fiber-optic probes. *Anal. Chem.* **1995**, *67*, 2858–2863.
5. Lu, X.; Lozano, R.; Shah, P. In-Situ Dissolution Testing Using Different UV Fiber Optic Probes and Instruments. *Dissolution Technol.* **2003**, *10* (4), 6–15.
6. Inman, G. W. Quantitative Assessment of Probe and Spectrometer Performance for a Multi-Channel CCD-based Fiber Optic Dissolution Testing System. *Dissolution Technol.* **2003**, *10* (4), 26–32.
7. Inman, G. W.; Wethington, E.; Baughman, K.; Horton, M. System Optimization for In Situ Fiber-Optic Dissolution testing. *Pharm. Technol.* **2001**, *10* (4), 92–100.
8. Bynum, K.; Roinestad, K.; Kassis, A.; Pocreva, J.; Gehriein, L.; Cheng, F.; Palermo P. Analytical Performance of a Fiber Optic Probes Dissolution System. *Dissolution Technol.* **2001**, *8* (4), 13–22.
9. Nir, I.; Johnson, B. D.; Johansson, J.; Schatz, C. Application of Fiber-Optic Dissolution Testing for Actual Products. *Pharm. Technol.* **2001**, *5* (2), 33–40.
10. Schatz, C.; Ulmschneider, M.; Altermatt, R.; Marrer, S. Evaluation of the Rainbow Dynamic Dissolution Monitor™ Semi-automatic Fiber Optic Dissolution Tester. *Dissolution Technol.* **2000**, *7* (4), 8–17.
11. Martin, C. A. Evaluation the Utility of Fiber Optic Analysis for Dissolution Testing of Drug Products. *Dissolution Technol.* **2003**, *10* (4), 37–39.
12. Wunderlich, M.; Way, T.; Dressman, J. Practical Considerations When Using Fiber Optics for Dissolution. *Dissolution Technol.* **2003**, *10* (4), 17–19.